

# Numerical Study of Turbulence Models in heat Transfer of a Confined and Submerged Jet Impingement using $Al_2O_3$ - water Nano Fluid

Amir H. Ghahremani<sup>1</sup>, Reza Saleh<sup>2</sup>

<sup>1</sup> (Department of mechanical engineering, Mashhad branch, Islamic Azad university, Mashhad, Iran)

<sup>2</sup> (Department of mechanical engineering, Mashhad branch, Islamic Azad university, Mashhad, Iran)

## Abstract

Fluids containing floating tiny particles in Nanometer scale, called Nano fluids, have a high potential in heat transfer augmentation. A numerical analysis of heat transfer in jet impingement of  $Al_2O_3$ -Water Nano fluid when turbulence models of Spalart-Allmaras,  $K-\epsilon$ ,  $K-\omega$  and Reynolds Stress are applied is studied. The experimental results found in laboratory for a confined and submerged circular jet impingement for Reynolds amounts of 20000, 40000, 60000 and 80000 when the distance between the nozzle and the wall is remained 2 mm constant is compared with numerical results and the weakness and strength of any of these 4 turbulence models is declared. The best results are found for  $K-\epsilon$  Realizable and Reynolds Stress models.

**Keywords:** Confined and submerged jet impingement, Nano fluid, Turbulence.

## I. INTRODUCTION

A fountain or a jet or a set of these fountains can be used to increase the heat transfer coefficient in cooling, heating and drying processes. These jets can impinge to a surface vertically. They can be used in convolving metal sheets, drying loom products and paper, cooling hot components of gas turbines and obviation of frigidity in airplane systems. Optimizing heat transfer facilities to reach higher efficiency requires increase in heat transfer rate. Common fluids in heat transfer are water, oil and ethylene glycol that have weak heat transfer nature [1]. Since conduction heat transfer of solid metals is more than fluids, it is expected to have higher convection heat transfer coefficient when metal particles or metal oxides are added to such base fluids [2]. The first study in this field goes back to several years ago. Maxwell [3] declared that the effective heat transfer coefficient of suspensions containing spherical particles increased when the volume fraction of solid particles is increased. However, until recently, all studies were limited in millimeter scale particles that could cause several Problems including fast precipitation, corrosion in stream pass and increase in pressure loss. These problems led to new applicable engineering fluids with high heat transfer

coefficient, called Nano fluids. Accomplished investigations for different forcible convection flows show that heat transfer rate in Nano fluids is depended on variety of parameters including the thickness of Nano fluid, size of Nano particles, Reynolds number, type of base fluid, the shape and the material of Nano particles.

To manifest how heat transfer rate is increased when Nano particles are added to a base fluid, several investigations are done about convection heat transfer. For instance, Zeinali Heris, Etemad et al. [4] considered Nano fluids convection heat transfer containing copper oxide and Aluminum oxide Nano particles for a constant temperature wall experimentally. Ebrahimnia-Bajestan, Niazmand et al. [5] studied numerical analysis for convection heat transfer of Nano fluids containing  $CuO$ ,  $Al_2O_3$  and carbon Nano tubes for a constant heat flux wall.

In previous declared investigations, laminar flow stream is considered and less research is done over forcible convection of Nano fluids in turbulent flow. Zuckerman and Lior [6] considered physics, correlations and numerical modeling for jet impingement heat transfer. Li, Xuan et al. [7] studied heat transfer for submerged single jet impingement using  $CuO$  water experimentally. Gao and Ewing [8] considered the effect of confinement in heat transfer of circular impinging jets exiting a long pipe. Shi, Ray et al. [9] studied computational heat transfer for a turbulent slot jet. An experimental and numerical analysis of applying turbulence models for a constant heat flux wall is also studied by Shi, Ray et al. [10]. In continue the effects of any of turbulence models regarding Spalart-Allmaras,  $K-\epsilon$ ,  $K-\omega$  and Reynolds Stress will be discussed based on numerical results.

## II. HYDRODYNAMIC AND GEOMETRY CONSIDERATION

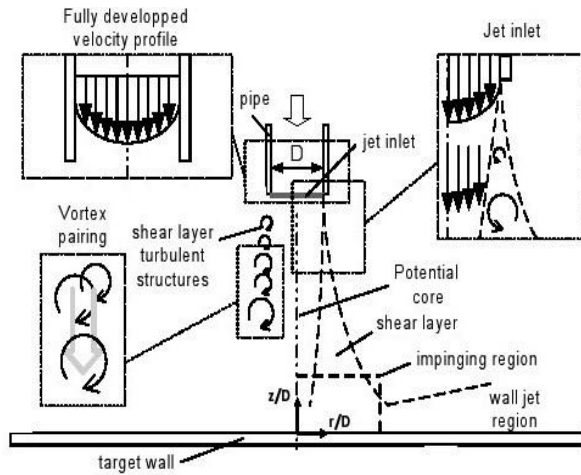


Fig. 1: Impinging Jet Specifications

Different specifications of a jet stream are shown in Fig. 1. Jets are usually sent throughout circular nozzles or rectangular cracks to a stagnant environment. In the stagnation region, the stream is affected by the target surface and its velocity in vertical ( $z$ ) and horizontal ( $r$ ) directions become lower and higher respectively. However, since the jet pulls the stagnant fluid of the ambient inside, horizontal acceleration can't increase to infinity; hence, accelerated fluid is transformed to a decelerated fluid in the stagnation region. As a result, components of the velocity parallel to the plane will reach to its maximum amount from zero on the wall and will again decrease to zero in the boundary of fluid and ambient. The leaving temperature is between the temperature of fluid leaving the nozzle and the surface temperature.

### III. CONVECTION HEAT TRANSFER

In provided equations, it is assumed that fluid leaves the nozzle with a constant velocity of  $V_e$  at a constant temperature of  $T_e$ .

A heating equilibrium ( $T_e = T_\infty$ ) is assumed, while convection heat transfer can occur in an impingement surface with constant temperature ( $T_s \neq T_e$ ). So, the cooling equation of Newton is defined as following:

$$q'' = h(T_s - T_\infty) \quad (1)$$

In the equation above it is assumed that the surface is fixed and the conditions are not affected by fluid turbulence.

A study for convection heat transfer in jet impingement is done by Shi, Ray et al.[11]. Fig. 2 depicts the contribution of local Nusselt number for a circular nozzle. Several experiments are done by Katti and Prabhu[12] for air jet impingement heat transfer for a circular nozzle to verify the accuracy of this figure.

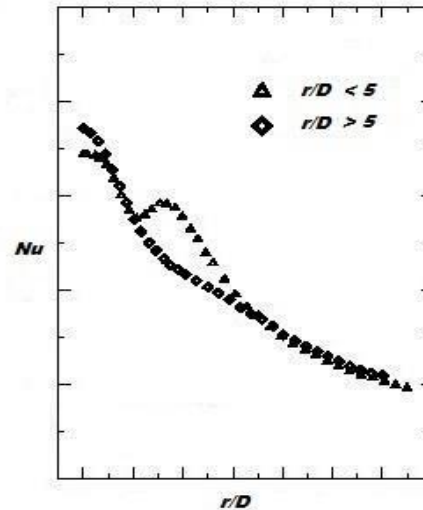


Fig. 2: Distribution of Local Nusselt Number using a Circular Nozzle for Close and Far Distance Between Nozzle and the Wall.

Based on Fig.2, for high distances between the nozzle and the wall, the Nusselt amount will decrease from its maximum in the stagnation region ( $\frac{r}{D} = 0$ ).

Fig.2 depicts another maximum peak for close distance between the nozzle and the target wall which is dependent on the jet's Reynolds number and is increased when the Reynolds number is increased and may ascend more than the first peak. The existence of the second maximum is related to the sudden increase in turbulence amount of the flow which is resulted due to changes in flow condition of stagnation region with positive acceleration to the wall fountain with negative acceleration[11]. Another maximum is seen which is ascribed to vortex generations in stagnation region and also conversion to turbulent fountain at the wall [13].

### IV. EFFECTIVE PROPERTIES OF NANO FLUIDS

To determine heat transfer coefficient and Nusselt number, it is required to find out the effective properties of Nano fluids regarding effective density, effective specific heat transfer coefficient, effective viscosity and effective conduction coefficient. Below equations are used for determination of these properties[14]:

$$\rho_{eff} = (1 - \phi)\rho_f + \phi\rho_p \quad (2)$$

$$(\rho C_p)_{eff} = (1 - \phi)(\rho C_p)_f + \phi(\rho C_p)_p \quad (3)$$

Maxwell[3]considered heat conduction for the mixture of a fluid and particles and determined an equation for effective conduction heat transfer coefficient defined as following:

$$K_{eff} = \frac{K_p + 2K_f + 2(K_p - K_f)\phi}{K_p + 2K_f - 2(K_p - K_f)\phi} K_f \quad (4)$$

Since the study of mutual effects of particles is condoned in Maxwell's investigations, this equation is only valid for low volume fraction mixtures.

## V. TURBULENCE MODELS

Turbulence is the state of fluid motion by random and three dimensional vortices. Since most of the industrial and engineering applications are turbulent, it plays an important role in most CFD studies. Turbulence models are classified based on the following categories:

- RANS- based models: the objectivity of this model is to calculate Reynolds stresses based on the following subdivisions:
  1. Linear eddy viscosity models: it includes algebraic models and one or two equation models.
  2. Non- Linear eddy viscosity models and algebraic stress models: this category includes explicit non-linear constitutive relation and V2-F models.
  3. Reynolds stress models (RSM).
- Large eddy simulations (LES).
- Detached eddy simulations (DES) and other hybrid models.
- Direct numerical simulations (DNS).

A useful turbulence model should be accurate, facile, economical and wide applicable. Many Turbulence models are based on Boussinesq approximation [15], corresponding turbulent stresses with mean strain rate in a tensor form defined as following:

$$\tau_{ij} = 2\mu_t S_{ij}^* - \frac{2}{3}\rho k \delta_{ij} \quad (5)$$

DNS is the most complete and accurate model in numerical simulations for impinging jets and transfer rates that solves full Navier-Stokes equations, continuity and mass diffusion using discrete units of time and space [6]. This model is suitable for laminar flows since the computational time to solve eddies for higher Reynolds numbers is increased [6]. Therefore, it is less reliable for turbulent jets like one studied in this article. To overcome this problem, LES models are taken into consideration showing better results in jet characteristics, effects of flow eddies upon the velocity and its promulgation. However, when  $Re > 1000$ , it requires more computer power and hence more time for reliable solutions.

RANS models are complex, having more terms and unknowns which require approximate modeling. In this numerical analysis four turbulence models of Spalart-Allmaras, K-ε, K-ω and Reynolds Stress are studied.

### A. Spalart-Allmaras model

Spalart and Allmaras [16] is a one equation model and a subdivision of linear eddy viscosity models considered as a part of RANS- based turbulence models. It solves a transport equation for a viscosity like variable of  $\tilde{\nu}$ , referred as Spalart-Allmaras model. The original model is as following:

$$\begin{aligned} \frac{\partial \tilde{\nu}}{\partial t} + u_j \frac{\partial \tilde{\nu}}{\partial x_j} &= C_{b1} [1 - f_{t2}] \tilde{S} \tilde{\nu} \\ &+ \frac{1}{\sigma} \{ \nabla \cdot [(\nu + \tilde{\nu}) \nabla \tilde{\nu}] + C_{b2} |\nabla \nu|^2 \} \\ &- \left[ C_{w1} f_w - \frac{C_{b1}}{k^2} f_{t2} \right] \left( \frac{\tilde{\nu}}{d} \right)^2 \\ &+ f_{t1} \Delta U^2 \quad (6) \end{aligned}$$

Where the constants and other auxiliary relations are defined by Spalart and Allmaras [16].

### B. K-ε Models

One of the most common linear eddy viscosity models in RANS based turbulence models is K-ε. It's a two equation model as it includes two transport equations to represent turbulence properties of flow which allows it to account for effects like convection and diffusion of turbulent energy. The variables are kinetic energy (K) and turbulent dissipation (ε). Three subdivisions of K-ε models are as following:

#### 1) Standard K-ε model

In this model the turbulent kinetic energy equation (K) is as following:

$$\begin{aligned} \frac{\partial(\rho k)}{\partial t} + \frac{\partial(\rho k u_i)}{\partial x_i} &= \frac{\partial}{\partial x_j} \left[ \left( \mu + \frac{\mu_t}{\sigma_k} \right) \frac{\partial k}{\partial x_j} \right] \\ &+ P_k + P_b - \rho \epsilon - Y_m + S_k \quad (7) \end{aligned}$$

The dissipation equation (ε) is as following:

$$\begin{aligned} \frac{\partial(\rho \epsilon)}{\partial t} + \frac{\partial(\rho \epsilon u_i)}{\partial x_i} &= \frac{\partial}{\partial x_j} \left[ \left( \mu + \frac{\mu_t}{\sigma_\epsilon} \right) \frac{\partial \epsilon}{\partial x_j} \right] \\ &+ C_{1\epsilon} \frac{\epsilon}{k} (P_k + C_{3\epsilon} P_b) - C_{2\epsilon} \rho \frac{\epsilon^2}{k} + S_\epsilon \quad (8) \end{aligned}$$

The constants and other auxiliary relations are defined by Launder and Sharma [17].

#### 2) RNG- K-ε Model

To consider the effects of smaller scales of motion, Launder and Sharma [18] developed renormalization group (RNG) to renormalize Navier-Stokes equations. Since eddy viscosity is determined from a single turbulence length scale in standard K-ε model, the turbulent diffusion occurs at specified scale. However, all scales of motion contribute in

turbulent diffusion. Therefore, this model studies different scales of motion through changes to the production term.

Transport equations for K and ε where buoyancy term is condoned are defined as following respectively:

$$\frac{\partial(\rho k)}{\partial t} + \frac{\partial(\rho k u_i)}{\partial x_i} = \frac{\partial}{\partial x_j} \left[ \left( \mu + \frac{\mu_t}{\sigma_k} \right) \frac{\partial k}{\partial x_j} \right] + P_k - \rho \epsilon \quad (9)$$

$$\frac{\partial(\rho \epsilon)}{\partial t} + \frac{\partial(\rho \epsilon u_i)}{\partial x_i} = \frac{\partial}{\partial x_j} \left[ \left( \mu + \frac{\mu_t}{\sigma_\epsilon} \right) \frac{\partial \epsilon}{\partial x_j} \right] + C_{1\epsilon} \frac{\epsilon}{k} P_k - C_{2\epsilon} \rho \frac{\epsilon^2}{k} \quad (10)$$

Where the constants and other auxiliary relations are defined by Launder and Sharma[18].

### 3) Realizable K-ε Model

In this model the transport equations are defined as following:

$$\frac{\partial(\rho k)}{\partial t} + \frac{\partial(\rho k u_i)}{\partial x_i} = \frac{\partial}{\partial x_j} \left[ \left( \mu + \frac{\mu_t}{\sigma_k} \right) \frac{\partial k}{\partial x_j} \right] + P_k + P_b - \rho \epsilon - Y_m + S_k \quad (11)$$

$$\frac{\partial(\rho \epsilon)}{\partial t} + \frac{\partial(\rho \epsilon u_i)}{\partial x_i} = \frac{\partial}{\partial x_j} \left[ \left( \mu + \frac{\mu_t}{\sigma_\epsilon} \right) \frac{\partial \epsilon}{\partial x_j} \right] + \rho C_{1\epsilon} S \epsilon - \rho C_{2\epsilon} \frac{\epsilon^2}{k + \sqrt{\nu \epsilon}} + C_{1\epsilon} \frac{\epsilon}{k} C_{3\epsilon} P_b + S_\epsilon \quad (12)$$

Where the constants and other auxiliary relations are defined by Launder and Sharma[19].

### C. . K-ω Models

K-ω models are two equation models including two extra transport equations to represent the turbulence properties of flow accounting for convection and diffusion of turbulent energy. The two variables that determine the scale of turbulence are turbulent kinetic energy (k) and the specific dissipation (ω). Two subdivisions of this model are defined in following:

#### 1) Wilcox K-Ω Model

The turbulence kinetic energy is defined as:

$$\frac{\partial k}{\partial t} + u_j \frac{\partial k}{\partial x_j} = \tau_{ij} \frac{\partial U_i}{\partial x_j} - \beta^* k \omega$$

$$+ \frac{\partial}{\partial x_j} \left[ (v + \sigma^* \nu_T) \frac{\partial k}{\partial x_j} \right] \quad (13)$$

The dissipation rate is also defined as following:

$$\frac{\partial \omega}{\partial t} + u_j \frac{\partial \omega}{\partial x_j} = \alpha \frac{\omega}{k} \tau_{ij} \frac{\partial U_i}{\partial x_j} - \beta \omega^2 + \frac{\partial}{\partial x_j} \left[ (v + \sigma \nu_T) \frac{\partial \omega}{\partial x_j} \right] \quad (14)$$

The constants and other auxiliary relations are defined by Wilcox[20].

#### 2) SST- K-ω Model

The SST- K-ω turbulence model is a two equation eddy viscosity model developed byMenter[21]. This model can be used as a low Reynolds turbulence model without any extra damping functions. This model reverts to K-ε behavior in the free stream and avoids the Wilcox's K-ω problem which is too sensitive to the inlet free stream turbulence properties.The turbulence kinetic energy is as following:

$$\frac{\partial k}{\partial t} + u_j \frac{\partial k}{\partial x_j} = \tau_{ij} \frac{\partial U_i}{\partial x_j} - \beta^* k \omega + \frac{\partial}{\partial x_j} \left[ (v + \sigma_k \nu_T) \frac{\partial k}{\partial x_j} \right] \quad (15)$$

And the dissipation rate is defined as:

$$\frac{\partial \omega}{\partial t} + u_j \frac{\partial \omega}{\partial x_j} = \alpha S^2 - \beta \omega^2 + \frac{\partial}{\partial x_j} \left[ (v + \sigma_\omega \nu_T) \frac{\partial \omega}{\partial x_j} \right] + 2(1 - F_1) \sigma_{\omega 2} \frac{1}{\omega} \frac{\partial k}{\partial x_i} \frac{\partial \omega}{\partial x_i} \quad (16)$$

Where the auxiliary relations and constants are defined byMenter[21].

#### 3) Reynolds Stress Model (RSM)

RSM models are higher level models originated by Launder, Reece et al.[22] which calculates shear stress directly while neglects eddy viscosity approach. The transport equations for Reynolds stress is as following:

$$\frac{\partial}{\partial t} (\rho \overline{u_i' u_j'}) + \frac{\partial}{\partial x_k} (\rho u_k \overline{u_i' u_j'}) = - \frac{\partial}{\partial x_k} \left[ \overline{\rho u_i' u_j' u_k'} + \overline{P' (\delta_{kj} u_i' + \delta_{ik} u_j')} \right]$$

$$\begin{aligned}
 & + \frac{\partial}{\partial x_k} \left[ \mu \frac{\partial}{\partial x_k} (\overline{u_i u_j}) \right] - \\
 & \rho \left( \overline{u_i u_k} \frac{\partial U_j}{\partial x_k} + \overline{u_j u_k} \frac{\partial U_i}{\partial x_k} \right) \\
 & - \rho \beta (g_i \overline{u_j \theta} + g_j \overline{u_i \theta}) \\
 & + P \left( \frac{\partial u_i}{\partial x_j} + \frac{\partial u_j}{\partial x_i} \right) - 2\mu \frac{\partial u_i}{\partial x_k} \frac{\partial u_j}{\partial x_k} \\
 & - 2\rho \Omega_k (\overline{u_j u_m} \epsilon_{ikm} + \overline{u_i u_m} \epsilon_{jkm}) \\
 & + S_{user} \tag{17}
 \end{aligned}$$

Where the Reynolds stress tensor is defined as following:

$$\rho \overline{u_i u_j} \tag{18}$$

### VI. EXPERIMENT CITATION

Nguyen, Galanis et al.[14]investigated heat transfer of a confined and submerged impingingjet experimentally using AL<sub>2</sub>O<sub>3</sub>. Water Nano fluid. The system was consisted of a 10 liter open reservoir and a high head centrifugal pump. A circular aluminum surface was heated by means of two standard 100 W nominal cartridge heaters. The diameter of the wall and the nozzle were 30 mm and 3 mm respectively. The average diameter of Nano particles was 36 nm. The experiment was done for three different distances of 2 mm, 5 mm and 10 mm between the nozzle and the wall. Three different solutions with the thickness of 0%, 2.8% and 6% was studied for each distance while Reynolds number range was chosen between 3800 and 88000. The thermo physical properties of AL<sub>2</sub>O<sub>3</sub> are as following:

$$\begin{aligned}
 \rho_p &= 3600 \text{ Kg}/\text{m}^3 \\
 (C_p)_p &= 773 \text{ J}/\text{Kg.K} \\
 K_p &= 36 \text{ W}/\text{m}^2.\text{K} \tag{19}
 \end{aligned}$$

### VII. MESH INDEPENDENCE STUDY

Every simulation needs proper meshing to determine reliable results. Therefore, the mesh type and the way it is used have a significant role in the accuracy of results. About 50 models are made to consider the accuracy of numerical studies. The best results are found when the number of cells is 1200 inwhich the vertical nodes is aggregated at the wall and expands toward the nozzle with the aspect ratio of 1.2. However, the horizontal space between the nodes was remained constant.

### VIII. DISCUSSION AND RESULTS

A numerical analysis regarding four turbulence models of Spalart-Allmaras, K-ε, K-ω and Reynolds Stress is done for heat transfer of a confined and submerged impinging jet using AL<sub>2</sub>O<sub>3</sub> – Water Nano fluid toward a fixed circular wall with constant heat flux using Fluent 2.3.26. When the fluid leaves the nozzle a shear flow is appeared at the boundary of the fluid jet which has low magnitude of oscillation and is the source of turbulence generation which gradually grows as it moves along the fluid path and thus creates larger eddies that have higher magnitude of oscillations. These shearing flows lead to the generation of vortices that become larger as the fluid leaves the nozzle toward the target wall. At the contact point of the jet and the wall, vortices are in their largest size having maximum oscillations which can lead to the generation of intense disarrangement that can carry copious amount of heat from the surface. This region is known as stagnation region. Since vortices have higher oscillation and turbulence in stagnation region, it's expected of more heat transfer rate than the center of the stagnation region where flow has the least velocity and oscillations. Based on the results shown in fig.3 for the variation of heat transfer coefficient, h, for different Reynolds, Spalart-Allmaras model is found to have the least deviation in comparison to experimental results; however, since this model solves the momentum equation by considering a variable for viscosity, it can't describe the dissipation rate and the jet spread properly. Therefore, it depicts undesirable results than when two or more equation models are studied.

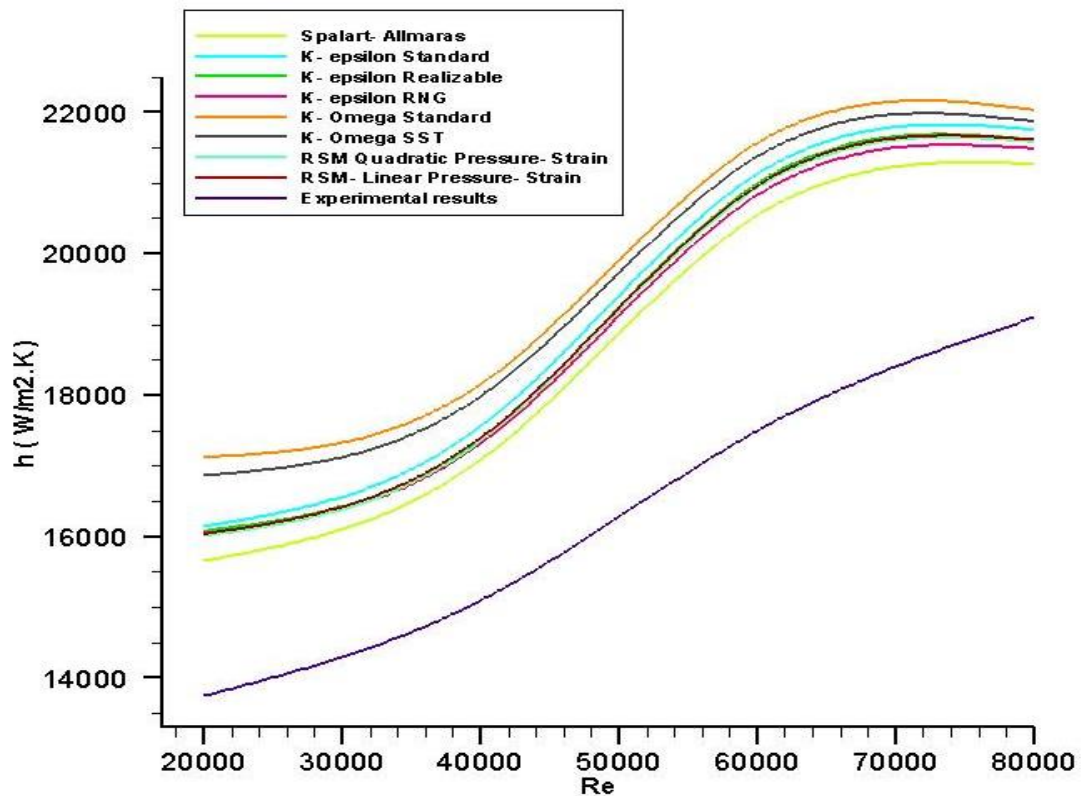


Fig.3: Variation of Heat Transfer Coefficient for Different Re Based on Experimental Results by Nguyen, Galanis Et Al.[14] as Well As Numerical Analysis Considering Turbulence Models For 2 Mm Distance Between Nozzle and The Target Wall.

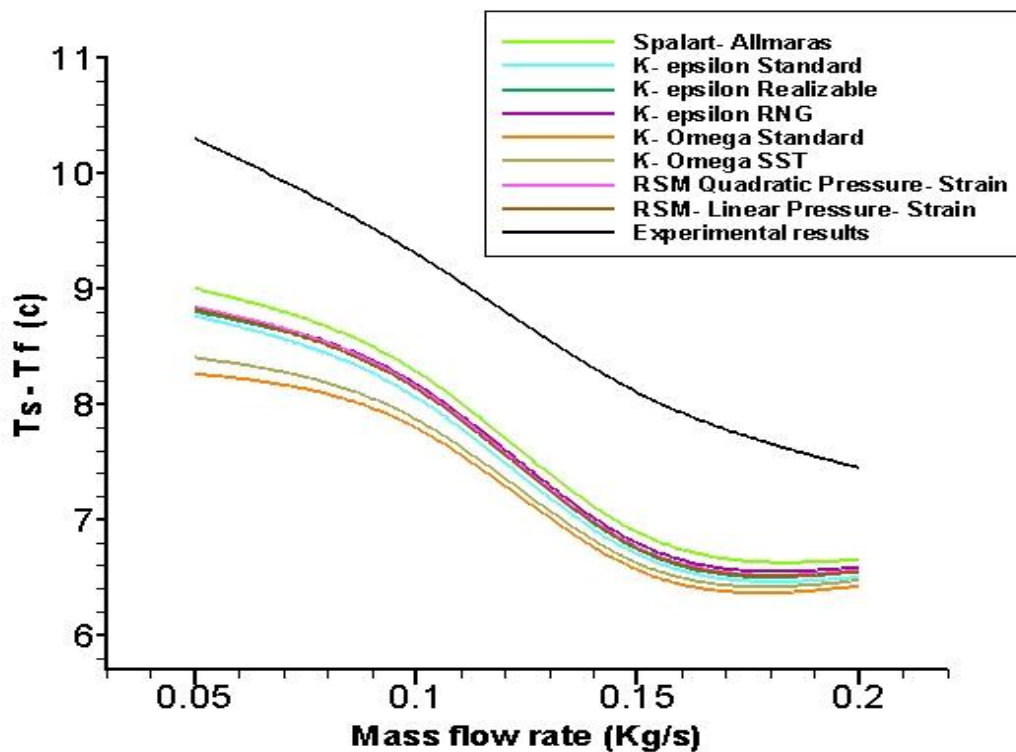


Fig.4: Variation of the Temperature Difference for Different Mass Flow Rate Based on Experimental Results Bynguyen, Galanis Et Al.[14] And Numerical Analysis Considering Turbulence Models For 2 Mm Distance Between Nozzle and The Target Wall.

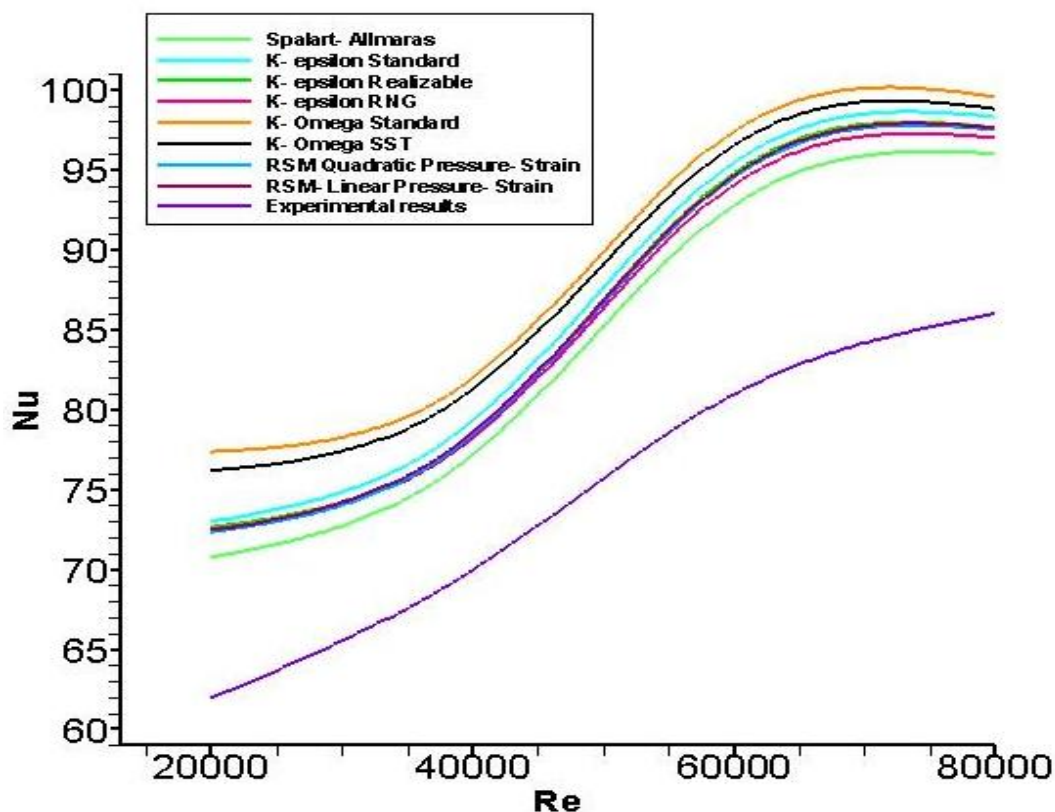


Fig.5: Variation Of Nu For Different Reynolds Based On Experimental Results By Nguyen, Galanis Et Al.[14]And Numerical Analysis Considering Turbulence Models For 2 Mm Distance Between Nozzle And The Target Wall.

Among two equation models of K- $\epsilon$  and K- $\omega$  considered in this investigation, K- $\epsilon$  models are found to give better results than K- $\omega$  models for which the standard K- $\epsilon$  model and RNG K- $\epsilon$  models give the most and the least deviation in comparison to experimental results respectively. Despite very close results of RNG and realizable K- $\epsilon$  models, K- $\epsilon$  realizable is superior to RNG K- $\epsilon$  model. A logical reason for this comparison can be due to extra terms in dissipation equation of standard and RNG K- $\epsilon$  models that are dependent on buoyancy production which depends on turbulence viscosity of fluid, turbulent Prandtl number and temperature gradient along the wall that are mainly related to the vortices magnitude when the jet hits the wall and therefore perform a dramatic influence in kinetic energy generation as well as dissipation rate that may estimate larger amounts for heat transfer coefficient at the stagnation region and along the wall. Since the buoyancy effect is condoned in RNG K- $\epsilon$  model, it can't predict the jet spreading properly. Despite the existence of production term in both standard and realizable K- $\epsilon$  models, standard K- $\epsilon$  model does not determine valid dissipation of round jets since it can't ascertain the buoyancy affects properly; however, in K- $\epsilon$  realizable model the existence of the term  $\rho C_2 \frac{\epsilon^2}{k + \sqrt{v\epsilon}}$  determines the buoyancy effects more logical since it considers the production of kinetic energy as well as viscosity and hence acts against over prediction of buoyancy

making it more reliable in determination of jet impingement properties. As it is shown in fig.3, based on experimental results by Nguyen, Galanis et al.[14], the heat transfer coefficient for Re=60000 is about 17500 W/m<sup>2</sup>.K while this amount was found around 20830 W/m<sup>2</sup>.K, 20994 W/m<sup>2</sup>.K and 21131 W/m<sup>2</sup>.K for RNG, realizable and standard models respectively and manifest errors about 19%,20% and 21% respectively in comparison to numerical results. Craft, Graham et al.[23] reported of error in the range of 15-20% for wall parallel velocity when applying K- $\epsilon$  models. Heyerichs and Pollard[24] also reported of Nu errors up to 50% when selecting K- $\epsilon$  models.

As it is shown in figures 3, 4 and 5, the maximum deviation was found for K- $\omega$  models. For instance, for Re=60000, the deviation between the numerical and experimental results was found around 23% which depicts an increase about 3% in average than the aberration for K- $\epsilon$  models. A reason for this deviation is that the kinetic energy dissipation coefficients are set based on experimental results rather than direct solution of velocity from the velocity field. This means that K- $\omega$  models over predict the impinging jet velocity and therefore the extent of stagnation region which yields to higher estimation of Nu and the heat transfer coefficient. Since heat transfer coefficient has direct relationship to Nu number and a reverse relationship with temperature, any increase in heat transfer coefficient yields to higher Nu amounts and therefore decreases

the temperature difference between the fluid and the contact wall surface. Heyerichs and Pollard[24] reported of over prediction of Nu up to 18% based on their studies. Park, Choi et al.[25] also reported an error up to 100% in local Nu number for higher Re amounts based on their investigation.

As it is seen in fig.5, Reynolds stress models depict close results to Realizable K- $\epsilon$  model. Since this model includes all terms of time, history, convection, diffusion and source, it can be counted as a reliable model for description of impinging jets. However, more number of iterations was found for convergence. This model predicts the Nu amount properly but can't estimate its location accurately [9]. Craft, Graham et al.[23] also reported an error up to 25% based on their studies.

Based on several researches done for impinging jets and applied turbulence models, it can be declared that all turbulence models can't determine the exact location and extent as well as the disarrangement of the jet flows, specifically in stagnation region which undertakes the most heat transfer share. On the other hand the numerical methods used in CFD solutions are not impeccable and all include errors and aberrations and therefore perform a dramatic influence on final results. The upwind method used in the simulation generates dramatic false phenomenon which adds more aberrations to the final result.

## IX. CONCLUSION

A numerical analysis of heat transfer in a confined and submerged jet impingement containing  $Al_2O_3$  – Water Nano fluid toward a constant heat flux wall when the distance between the nozzle and the wall was remained 2 mm is studied. Four turbulence models of spalart-Allmaras, K- $\epsilon$ , K- $\omega$  and Reynolds Stress Models were studied for Reynolds number range from almost 20000 to 80000. The best results were found for Realizable K- $\epsilon$  model as well as Reynolds Stress model (RSM). However, despite RSM is the most complete model, its time taking process and the more CPU effort makes it unfavorable to use. In addition, the worst results were found for K- $\omega$  models. Based on several studies and investigations in different literatures, it can be said

## REFERENCES

- [1] Bayat, J. and A. Nikseresh, Investigation of the different base fluid effects on the nanofluids heat transfer and pressure drop. Heat and Mass Transfer, 2011. 47(9): p. 1089-1099.
- [2] Choi, S.U.S., Enhancing thermal conductivity of fluids with nanoparticles. ASME-Publications-Fed, 1995. 231: p. 99-106.
- [3] Maxwell, J.C., A treatise on electricity and magnetism. Vol. 1. 1881: Clarendon press.
- [4] Zeinali Heris, S., S.G. Etemad, and M. Nasr Esfahany, Experimental investigation of oxide nanofluids laminar flow convective heat transfer. International Communications in Heat and Mass Transfer, 2006. 33(4): p. 529-535.
- [5] Ebrahimnia-Bajestan, E., et al., Numerical investigation of effective parameters in convective heat transfer of nanofluids flowing under a laminar flow regime. International Journal of Heat and Mass Transfer, 2011. 54: p. 4376-4388.
- [6] Zuckerman, N. and N. Lior, Jet Impingement Heat Transfer: Physics, Correlations, and Numerical Modeling. Advances in Heat Transfer, 2006. 39.

that all turbulence models as well as numerical solutions have drawbacks; however, they are accurate enough to rely on their results. Impinging jets are time dependent and steady state simulations do not represent the physics properly.

## NOMENCLATURE

$T_s$	Wall temperature
$T_\infty$	Fluid temperature
$V_e$	Fluid velocity leaving the nozzle
$Y_m$	Fluctuation dilatation in compressible flow
$z$	Distance between nozzle and the wall
$C_p$	Specific heat transfer coefficient
$D$	Nozzle diameter
$h$	Surface convection heat transfer coefficient
$K_{eff}$	Effective conduction heat transfer coefficient
$K_f$	Conduction heat transfer coefficient of base fluid
$K_p$	Conduction heat transfer coefficient of Nano particles
$Nu$	Nozzle Nusselt number
$P_b$	Production of buoyancy
$P_k$	Production of kinetic energy $q''$ Total heat flux
$r$	Target wall radius
$Re$	Nozzle Reynolds number
$S_k$	Source of kinetic energy
$S_\epsilon$	Source of dissipation
$S_{ij}^*$	Trace-less mean strain rate tensor.
$T_e$	Fluid temperature leaving the nozzle

## GREEK SYMBOLS

$\epsilon$	Dissipation
$\rho$	Density
$\beta$	Thermal expansion
$\rho_{eff}$	Effective density
$\rho_f$	Fluid density
$\rho_p$	Nano Particles density
$\varphi$	Nano Particles mass fraction
$\nu_T$	Turbulent Kinematic viscosity
$\omega$	Specific dissipation
$\tau_{ij}$	Turbulence stress tensor
$\mu_t$	Turbulence dynamic viscosity

- [7] Li, Q., Y. Xuan, and F. Yu, Experimental investigation of submerged single jet impingement using CuO-water nanofluid. *Applied Thermal Engineering*, 2012. 36(0): p. 426-433.
- [8] Gao, N. and D. Ewing, Investigation of the effect of confinement on the heat transfer to round impinging jets exiting a long pipe. *International Journal of Heat and Fluid Flow*, 2006. 27(1): p. 33-41.
- [9] Shi, Y., M.B. Ray, and A.S. Mujumdar, Computational study of impingement heat transfer under a turbulent slot jet. *Industrial & engineering chemistry research*, 2002. 41(18): p. 4643-4651.
- [10] Bovo, M., S. Etemad, and L. Davidson, On The Numerical Modeling Of Impinging Jet Heat Transfer. *Int. Symp. on Convective Heat and Mass Transfer in Sustainable Energy*, 2009.
- [11] Martin, H., P.H. James, and F.I. Thomas, Heat and Mass Transfer between Impinging Gas Jets and Solid Surfaces, in *Advances in Heat Transfer*. 1977, Elsevier. p. 1-60.
- [12] Katti, V. and S.V. Prabhu, Experimental study and theoretical analysis of local heat transfer distribution between smooth flat surface and impinging air jet from a circular straight pipe nozzle. *International Journal of Heat and Mass Transfer*, 2008. 51(17): p. 4480-4495.
- [13] Popiel, C.O. and L. Boguslawski, Mass or heat transfer in impinging single, round jet emitted by a bell-shaped nozzle and sharp-ended orifice. *Heat Transfer*, 1986. 3: p. 1187-1192.
- [14] Nguyen, C.T., et al., An experimental study of a confined and submerged impinging jet heat transfer using Al<sub>2</sub>O<sub>3</sub>-water nanofluid. *International Journal of Thermal Sciences*, 2009. 48(2): p. 401-411.
- [15] Boussinesq, J., *Essai sur la théorie des eaux courantes*. Vol. 2. 1877: Imprimerie nationale.
- [16] Spalart, P.R. and S.R. Allmaras, A one equation turbulence model for aerodynamic flows. *AIAA journal*, 1992. 94.
- [17] Launder, B.E. and B.I. Sharma, Application of the energy-dissipation model of turbulence to the calculation of flow near a spinning disc. *Letters in heat and mass transfer*, 1974. 1(2): p. 131-137.
- [18] Yakhot, V., et al., Development of turbulence models for shear flows by a double expansion technique. *Physics of Fluids A: Fluid Dynamics (1989-1993)*, 1992. 4(7): p. 1510-1520.
- [19] Shih, T.-H., et al., A New k-epsilon Eddy-Viscosity Model for High Reynolds Number Turbulent Flows. *Computers & Fluids*, 1995. 24(3): p. 227-238.
- [20] Wilcox, D.C., *Turbulence modeling for CFD*. La Canada, California: DCW Industries. 1998, Inc.
- [21] Menter, F.R., Zonal two equation k-turbulence models for aerodynamic flows. *AIAA paper*, 1993. 2906.
- [22] Launder, B.E., G. Reece, Jr., and W. Rodi, Progress in the development of a Reynolds-stress turbulence closure. *Journal of fluid mechanics*, 1975. 68(03): p. 537-566.
- [23] Craft, T.J., L.J.W. Graham, and B.E. Launder, Impinging jet studies for turbulence model assessment-II. An examination of the performance of four turbulence models. *International Journal of Heat and Mass Transfer*, 1993. 36(10): p. 2685-2697.
- [24] Hejranfar, K. and A. Pollard, Heat transfer in separated and impinging turbulent flows. *International Journal of Heat and Mass Transfer*, 1996. 39(12): p. 2385-2400.
- [25] Park, T.H., et al., Streamline upwind numerical simulation of two-dimensional confined impinging slot jets. *International Journal of Heat and Mass Transfer*, 2003. 46(2): p. 251-262.